JOURNAL OF THEORETICAL
AND APPLIED MECHANICS
49, 2, pp. 439-455, Warsaw 2011

MATHEMATICAL MODELLING OF A RECTANGULAR SANDWICH PLATE WITH A METAL FOAM CORE

Ewa Magnucka-Blandzi
Poznań University of Technology, Institute of Mathematics, Poznań, Poland
e-mail: ewa.magnucka-blandzi@put.poznan.pl

The subject of the paper is a simply supported rectangular sandwich plate. The plate is compressed in plane. It is assumed that the plate under consideration is symmetrical in build and consists of two isotropic facings and a core. The middle plane of the plate is its symmetry plane. The core is made of a metal foam with properties varying across its thickness. The porous-cellular metal as a core of the three layered plate is of continuous structure, while its mechanical properties are isotropic. Dimensionless coefficients are introduced to compensate for this.
The field of displacements and geometric relationships are assumed. This non-linear hypothesis is generalization of the classical hypotheses, in particular, the broken-line hypothesis. The principle of stationarity of the total potential energy of the compressed sandwich plate is used and a system of differential equations is formulated. This system is approximately solved. The forms of unknown functions are assumed, which satisfy boundary conditions for supports of the plate. Critical loads for a family of sandwich plates are numerically determined. Results of the calculation are shown in figures.

Key words: sandwich plate, critical load, metal foam core

1. Introduction

In the last years, composite beams, plates and shells are applied in mechanical engineering, particularly in vehicles and building engineering. Strength and buckling problems of sandwich structures are studied in practice since the mid of the 20th century. There are monograph works devoted to this topic, e.g. Plantema (1966), Volmir (1967), Grigolyuk and Chulkov (1973), Noor *et al.* (1996), Wang *et al.* (2000), Magnucki and Ostwald (2001). These monograph papers demonstrate the development of research of strength and buckling of classical sandwich beams, plates, and shells with homogeneous cores. Contemporary studies of the strength and stability problems of classical sandwich structures are presented by Kotełko and Mania (2005) or Ohga *et al.* (2005). The sandwich structures with metal foam cores are only rarely dealt within such a wide field of investigation. Magnucki and Stasiewicz (2004a,b), Malinowski and Magnucki (2005), Magnucki *et al.* (2006), carried out analytical investigations of strength and stability of porous-cellular beams, plates and cylindrical shells with consideration of a non-linear hypothesis of the deformation of flat cross section of the structures. The first hypothesis of displacements and equilibrium equations of three-layered constructions were formulated in the middle of 20th century and it was presented by Grigolyuk and Chulkov (1973). Wang *et al.* (2000) discussed the higher order hypotheses including shear deformation of beams and plates. Carrera (2000, 2001, 2003) formulated the zig-zag hypotheses for multilayered plates. Carrera *et al.* (2008) presented the static analysis of functionally graded material plates subjected to transverse mechanical loadings. Debowski and Magnucki (2006) formulated a nonlinear hypothesis of deformation for porous rectangular plates with using trygonometric functions. Kasprzak and Ostwald (2006) presented a generalization of the hypotheses of deformations. Banhart (2001), Bart-Smith *et al.* (2001), and Hohe and Becker (2002) presented the manufacture, characterization and application of cellular metals and metal foams for sandwich structures. Magnucka-Blandzi and Magnucki (2007) and Magnucki and Magnucka-Blandzi (2006) described the strength and stability problems of a sandwich beam with a porous-cellular core and its effective design. Pandit *et al.* (2008) presented an improved higher order zigzag theory and applied it to study the buckling of laminated sandwich plates. The variation of in-plane displacements through the thickness direction is assumed to be cubic for both the face sheets and the core, while transverse displacement is assumed to vary quadratically within the core but it remains constant over the face sheets. Apetre *et al.* (2008) investigated several available sandwich beam theories for their suitability of application to one-dimensional sandwich plates with functionally graded cores. Two equivalent single-layer theories based on assumed displacements, a higher-order theory, and the Fourier-Galerkin method were compared. The variation of core Young's modulus was presented by a differentiable function in the thickness coordinate, but the Poisson's ratio was kept constant.

The subject of the paper is a simply-supported rectangular sandwich plate with a metal foam core. The paper is an improvement and continuation of the papers by Magnucka-Blandzi and Magnucki (2007), Magnucki and Magnucka-Blandzi (2006), Magnucka-Blandzi (2008, 2009), Magnucka-Blandzi and Wasilewicz (2009) and Magnucka-Blandzi (2010).

The plate with sizes a, b and the thickness $2t_f + t_c$ carries a uniform compressive forces N_x^0, N_y^0 (Fig. 1).

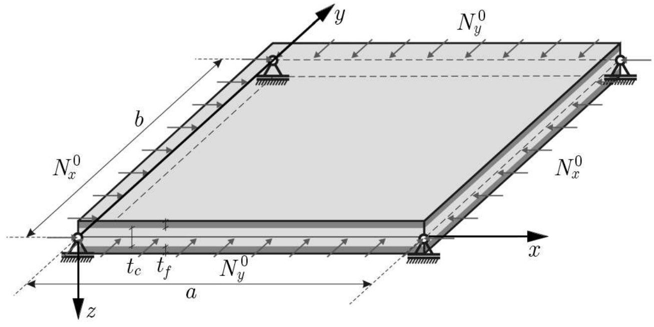

Fig. 1. Scheme of the sandwich plate under compression

2. Physical model of the sandwich plate

The sandwich plate with a metal foam core is studied. Metal faces of thickness t_f are isotropic of Young's modulus E_f and Poisson's ratio ν_f . The metal foam core of thickness t_c is assumed as isotropic with varying mechanical properties (Fig. 2), but Poisson's ratio ν_c is kept constant.

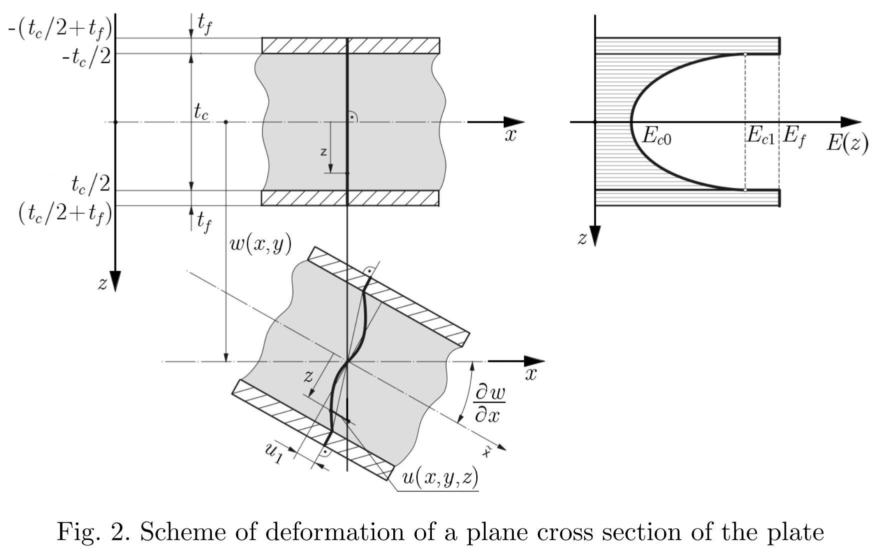

Fig. 2. Scheme of deformation of a plane cross section of the plate

The minimal value of Young's modulus occurs in the middle plane of the plate and the maximal value at its top and bottom surfaces of the core. The core is porous inside with the degree of porosity varying in the normal direction. The moduli of elasticities are defined as follows

$$E_c(\zeta) = E_{c1}[1 - e_0 \cos(\pi\zeta)] \qquad G_c(\zeta) = G_{c1}[1 - e_0 \cos(\pi\zeta)] \tag{2.1}$$

where

e_0	–	coefficient of the core porosity, $e_0 = 1 - E_{c0}/E_{c1}$
E_{c0}, E_{c1}	–	Young's moduli at $z = 0$ and $z = \pm t_c/2$, respectively
G_{c0}, G_{c1}	–	shear moduli for $z = 0$ and $z = \pm t_c/2$, respectively
G_{cj}	–	relationship between the moduli of elasticity for $j = 0, 1$, $G_{cj} = E_{cj}/[2(1 + \nu)]$
ν_f, ν_c	–	Poisson's ratios for faces and the core
ζ	–	dimensionless coordinate, $\zeta = z/t_c$
t_f	–	thickness of each face
t_c	–	thickness of the core

Displacements of points laying on the cross-section of the plate arise from the assumed hypothesis of deformation (Fig. 2). The field of displacement is defined:

— the upper face: $-(0.5 + x_1) \leqslant \zeta \leqslant -0.5$

$$\begin{aligned} u(x, y, \zeta) &= -t_c\Big[\zeta\frac{\partial w}{\partial x} + \psi_0(x, y) - \frac{1}{\pi}\psi_1(x, y)\Big] \\ v(x, y, \zeta) &= -t_c\Big[\zeta\frac{\partial w}{\partial y} + \phi_0(x, y) - \frac{1}{\pi}\phi_1(x, y)\Big] \end{aligned} \tag{2.2}$$

where $\psi_1(x, t) = u_1(x, t)/t_c$

— the core: $-0.5 \leqslant \zeta \leqslant 0.5$

$$\begin{aligned} u(x, y, \zeta) &= -t_c\Big\{\zeta\Big[\frac{\partial w}{\partial x} - 2\psi_0(x, y)\Big] + \frac{1}{\pi}\psi_1(x, y)\sin(\pi\zeta)\Big\} \\ v(x, y, \zeta) &= -t_c\Big\{\zeta\Big[\frac{\partial w}{\partial y} - 2\phi_0(x, y)\Big] + \frac{1}{\pi}\phi_1(x, y)\sin(\pi\zeta)\Big\} \end{aligned} \tag{2.3}$$

— the lower face: $0.5 \leqslant \zeta \leqslant 0.5 + x_1$

$$\begin{aligned} u(x, y, \zeta) &= -t_c\Big[\zeta\frac{\partial w}{\partial x} - \psi_0(x, y) + \frac{1}{\pi}\psi_1(x, y)\Big] \\ v(x, y, \zeta) &= -t_c\Big[\zeta\frac{\partial w}{\partial y} - \phi_0(x, y) + \frac{1}{\pi}\phi_1(x, y)\Big] \end{aligned} \tag{2.4}$$

where $x_1 = t_f/t_c$.

There are five unknown autonomous functions: $w(x,y)$ – deflection, $\psi_0(x,y)$, $\psi_1(x,y)$, $phi_0(x,y)$, $\phi_1(x,y)$ – dimensionless functions of displacements. In the particular case $\psi_0(x,y) = \psi_1(x,y) = \phi_0(x,y) = \phi_1(x,y) = 0$, the field of displacements u, v is linear the Kirchhoff-Love hypothesis. Functions $\psi_0(x,y), \psi_1(x,y), \phi_0(x,y), \phi_1(x,y)$ extend the linear classical hypothesis. In the classical theory, thea shear force is equal to zero (it follows from this linear theory), but in the proposed non-linear hypothesis the shear force does not equal zero, which corresponds with the facts.

The geometric relationships, i.e. components of the strain for each layer of the plate, are:
— the upper face: $-(0.5 + x_1) \leqslant \zeta \leqslant -0.5$

$$
\begin{aligned}
\varepsilon_x^{(f1)} &= \frac{\partial u}{\partial x} = -t_c\Big(\zeta\frac{\partial^2 w}{\partial x^2} + \frac{\partial \psi_0}{\partial x} - \frac{1}{\pi}\frac{\partial \psi_1}{\partial x}\Big)\\
\varepsilon_y^{(f1)} &= \frac{\partial v}{\partial y} = -t_c\Big(\zeta\frac{\partial^2 w}{\partial y^2} + \frac{\partial \phi_0}{\partial y} - \frac{1}{\pi}\frac{\partial \phi_1}{\partial y}\Big)\\
\gamma_{xz}^{(f1)} &= \frac{1}{t_c}\frac{\partial u}{\partial \zeta} + \frac{\partial w}{\partial x} = 0\\
\gamma_{yz}^{(f1)} &= \frac{1}{t_c}\frac{\partial v}{\partial \zeta} + \frac{\partial w}{\partial y} = 0\\
\gamma_{xy}^{(f1)} &= \frac{\partial u}{\partial y} + \frac{\partial v}{\partial x} =\\
&= -t_c\Big[2\zeta\frac{\partial^2 w}{\partial x \partial y} + \frac{\partial \psi_0}{\partial y} + \frac{\partial \phi_0}{\partial x} - \frac{1}{\pi}\Big(\frac{\partial \psi_1}{\partial y} + \frac{\partial \phi_1}{\partial x}\Big)\Big]
\end{aligned}
\tag{2.5}
$$

— the core: $-0.5 \leqslant \zeta \leqslant 0.5$

$$
\begin{aligned}
\varepsilon_x^{(c)} &= \frac{\partial u}{\partial x} = -t_c\Big[\zeta\Big(\frac{\partial^2 w}{\partial x^2} - 2\frac{\partial \psi_0}{\partial x}\Big) + \frac{1}{\pi}\frac{\partial \psi_1}{\partial x}\sin(\pi\zeta)\Big]\\
\varepsilon_y^{(c)} &= \frac{\partial v}{\partial y} = -t_c\Big[\zeta\Big(\frac{\partial^2 w}{\partial y^2} - 2\frac{\partial \phi_0}{\partial y}\Big) + \frac{1}{\pi}\frac{\partial \phi_1}{\partial y}\sin(\pi\zeta)\Big]\\
\gamma_{xz}^{(c)} &= \frac{1}{t_c}\frac{\partial u}{\partial \zeta} + \frac{\partial w}{\partial x} = 2\psi_0(x,y) - \psi_1(x,y)\cos(\pi\zeta)\\
\gamma_{yz}^{(c)} &= \frac{1}{t_c}\frac{\partial v}{\partial \zeta} + \frac{\partial w}{\partial y} = 2\phi_0(x,y) - \phi_1(x,y)\cos(\pi\zeta)\\
\gamma_{xy}^{(c)} &= \frac{\partial u}{\partial y} + \frac{\partial v}{\partial x} =\\
&= -t_c\Big[2\zeta\Big(\frac{\partial^2 w}{\partial x \partial y} - \frac{\partial \psi_0}{\partial y} - \frac{\partial \phi_0}{\partial x}\Big) + \frac{1}{\pi}\Big(\frac{\partial \psi_1}{\partial y} + \frac{\partial \phi_1}{\partial x}\Big)\sin(\pi\zeta)\Big]
\end{aligned}
\tag{2.6}
$$

— the lower face: $0.5 \leqslant \zeta \leqslant 0.5 + x_1$

$$\begin{aligned}
\varepsilon_x^{(f2)} &= \frac{\partial u}{\partial x} = -t_c\Big(\zeta\frac{\partial^2 w}{\partial x^2} - \frac{\partial \psi_0}{\partial x} + \frac{1}{\pi}\frac{\partial \psi_1}{\partial x}\Big)\\
\varepsilon_y^{(f2)} &= \frac{\partial v}{\partial y} = -t_c\Big(\zeta\frac{\partial^2 w}{\partial y^2} - \frac{\partial \phi_0}{\partial y} + \frac{1}{\pi}\frac{\partial \phi_1}{\partial y}\Big)\\
\gamma_{xz}^{(f2)} &= \frac{1}{t_c}\frac{\partial u}{\partial \zeta} + \frac{\partial w}{\partial x} = 0\\
\gamma_{yz}^{(f2)} &= \frac{1}{t_c}\frac{\partial v}{\partial \zeta} + \frac{\partial w}{\partial y} = 0\\
\gamma_{xy}^{(f2)} &= \frac{\partial u}{\partial y} + \frac{\partial v}{\partial x} =\\
&= -t_c\Big[2\zeta\frac{\partial^2 w}{\partial x \partial y} - \frac{\partial \psi_0}{\partial y} - \frac{\partial \phi_0}{\partial x} + \frac{1}{\pi}\Big(\frac{\partial \psi_1}{\partial y} + \frac{\partial \phi_1}{\partial x}\Big)\Big]
\end{aligned} \tag{2.7}$$

Stresses in all layers of the plate, with respect to Hooke's law, are as follows:
— the upper or the lower face

$$\begin{aligned}
\sigma_x^{(fi)} &= \frac{E_f}{1-\nu_f^2}\Big(\varepsilon_x^{(fi)} + \nu_f\varepsilon_y^{(fi)}\Big)\\
\sigma_y^{(fi)} &= \frac{E_f}{1-\nu_f^2}\Big(\varepsilon_y^{(fi)} + \nu_f\varepsilon_x^{(fi)}\Big)\\
\tau_{xy}^{(fi)} &= G_f\gamma_{xy}^{(fi)}
\end{aligned} \tag{2.8}$$

— the core

$$\begin{aligned}
\sigma_x^{(c)} &= \frac{E_{c1}}{1-\nu_c^2}[1 - e_0\cos(\pi\zeta)]\Big(\varepsilon_x^{(c)} + \nu_c\varepsilon_y^{(c)}\Big)\\
\sigma_y^{(c)} &= \frac{E_{c1}}{1-\nu_c^2}[1 - e_0\cos(\pi\zeta)]\Big(\varepsilon_y^{(c)} + \nu_c\varepsilon_x^{(c)}\Big)\\
\tau_{xy}^{(c)} &= G_{c1}[1 - e_0\cos(\pi\zeta)]\gamma_{xy}^{(c)}\\
\tau_{xz}^{(c)} &= G_{c1}[1 - e_0\cos(\pi\zeta)]\gamma_{xz}^{(c)}\\
\tau_{yz}^{(c)} &= G_{c1}[1 - e_0\cos(\pi\zeta)]\gamma_{yz}^{(c)}
\end{aligned} \tag{2.9}$$

The deflection for each layer of the plate is the same and does not depend on the z coordinate, which means

$$w(x, y, z) = w(x, y) \tag{2.10}$$

3. Mathematical model of the sandwich plate

Equations of stability are based on the principle of minimum of the total potential energy

$$\delta(U_\varepsilon - W) = 0 \tag{3.1}$$

U_ε is the energy of elastic strain, where $U_\varepsilon = U_\varepsilon^{(f1)} + U_\varepsilon^{(c)} + U_\varepsilon^{(f2)}$

$$\begin{aligned}
U_\varepsilon^{(f1)} &= \frac{t_c}{2}\int\limits_0^a\int\limits_0^b\int\limits_{-(\frac{1}{2}+x_1)}^{-\frac{1}{2}} \Big(\sigma_x^{(f1)}\varepsilon_x^{(f1)} + \sigma_y^{(f1)}\varepsilon_y^{(f1)} + \tau_{xy}^{(f1)}\gamma_{xy}^{(f1)}\Big)\, d\zeta\, dy\, dx \\
U_\varepsilon^{(c)} &= \frac{t_c}{2}\int\limits_0^a\int\limits_0^b\int\limits_{-\frac{1}{2}}^{\frac{1}{2}} \Big(\sigma_x^{(c)}\varepsilon_x^{(c)} + \sigma_y^{(c)}\varepsilon_y^{(c)} + \tau_{xy}^{(c)}\gamma_{xy}^{(c)} + \tau_{xz}^{(c)}\gamma_{xz}^{(c)} + \tau_{yz}^{(c)}\gamma_{yz}^{(c)}\Big)\, d\zeta\, dy\, dx \\
U_\varepsilon^{(f2)} &= \frac{t_c}{2}\int\limits_0^a\int\limits_0^b\int\limits_{\frac{1}{2}}^{\frac{1}{2}+x_1} \Big(\sigma_x^{(f2)}\varepsilon_x^{(f2)} + \sigma_y^{(f2)}\varepsilon_y^{(f2)} + \tau_{xy}^{(f2)}\gamma_{xy}^{(f2)}\Big)\, d\zeta\, dy\, dx
\end{aligned} \tag{3.2}$$

$U_\varepsilon^{(f1)}$ – energy of the upper face, $U_\varepsilon^{(c)}$ – energy of the core, $U_\varepsilon^{(f2)}$ – energy of the lower face. W is the work of the compressive force

$$W = \frac{1}{2}\int\limits_0^a\int\limits_0^b \Big[N_x^0\Big(\frac{\partial w}{\partial x}\Big)^2 + N_y^0\Big(\frac{\partial w}{\partial y}\Big)^2\Big]\, dy\, dx \tag{3.3}$$

where $N_x^0 = kN_0$, $N_y^0 = (1-k)N_0$, $(0 \leqslant k \leqslant 1)$.

Basing on the principle of minimum of the total potential energy, Eq. (3.1), a system of five differential stability equations is obtained

$$\begin{aligned}
(\delta w) \qquad & \frac{E_{c1}t_c^3}{1-\nu_c^2}\Big[(2\alpha_{11}c_{20} + c_{11})\Big(\frac{\partial^4 w}{\partial x^4} + \frac{\partial^4 w}{\partial y^4}\Big) + \\
& +(4\alpha_{11}\nu_f c_{20} + 4\alpha_{11}c_{21} + 2c_{11})\frac{\partial^4 w}{\partial x^2 \partial y^2} - (\alpha_{12}c_{20} + 2c_{11}) \cdot \\
& \cdot\Big(\frac{\partial^3 \psi_0}{\partial x^3} + \frac{\partial^3 \phi_0}{\partial y^3}\Big) - (\alpha_{12}\nu_f c_{20} + \alpha_{12}c_{21} + 2c_{11})\cdot
\end{aligned} \tag{3.4}$$

$$\cdot\Big(\frac{\partial^3\psi_0}{\partial x\partial y^2}+\frac{\partial^3\phi_0}{\partial x^2\partial y}\Big)+\Big(\frac{1}{\pi}\alpha_{12}c_{20}+c_{15}\Big)\Big(\frac{\partial^3\psi_1}{\partial x^3}+\frac{\partial^3\phi_1}{\partial y^3}\Big)+$$
$$+\Big(\frac{1}{\pi}\alpha_{12}\nu_f c_{20}+\frac{1}{\pi}\alpha_{12}c_{21}+c_{15}\Big)\Big(\frac{\partial^3\psi_1}{\partial x\partial y^2}+\frac{\partial^3\phi_1}{\partial x^2\partial y}\Big)\Big]=$$
$$=-N_x^0\frac{\partial^2 w}{\partial x^2}-N_y^0\frac{\partial^2 w}{\partial y^2}$$

$$(\delta\psi_0)\qquad \frac{2t_c^2}{1-\nu_c}\Big\{(\alpha_{12}c_{20}+2c_{11})\frac{\partial^3 w}{\partial x^3}+(\alpha_{12}\nu_f c_{20}+\alpha_{12}c_{21}+2c_{11})\cdot$$
$$\cdot\frac{\partial^3 w}{\partial x\partial y^2}-(2x_1c_{20}+4c_{11})\frac{\partial^2\psi_0}{\partial x^2}-[x_1c_{21}+2c_{11}(1-\nu_c)]\cdot$$
$$\cdot\frac{\partial^2\psi_0}{\partial y^2}+\Big(\frac{2}{\pi}x_1c_{20}+2c_{15}\Big)\frac{\partial^2\psi_1}{\partial x^2}+\Big[\frac{1}{\pi}x_1c_{21}+c_{15}(1-\nu_c)\Big]\cdot \tag{3.5}$$
$$\cdot\frac{\partial^2\psi_1}{\partial y^2}-[2x_1\nu_f c_{20}+x_1x_{21}+2c_{11}(1+\nu_c)]\frac{\partial^2\phi_0}{\partial x\partial y}+$$
$$+\Big[\frac{2}{\pi}x_1\nu_f c_{20}+\frac{1}{\pi}x_1c_{21}+c_{15}(1+\nu_c)\Big]\frac{\partial^2\phi_1}{\partial x\partial y}\Big\}+$$
$$+4c_0\psi_0-c_{16}\psi_1=0$$

$$(\delta\psi_1)\qquad \frac{t_c^2}{1-\nu_c}\Big\{-\Big(\frac{2}{\pi}\alpha_{12}c_{20}+2c_{15}\Big)\frac{\partial^3 w}{\partial x^3}+$$
$$-\Big(\frac{2}{\pi}\alpha_{12}\nu_f c_{20}+\frac{2}{\pi}\alpha_{12}c_{21}+2c_{15}\Big)\frac{\partial^3 w}{\partial x\partial y^2}+$$
$$+\Big(\frac{4}{\pi}x_1c_{20}+4c_{15}\Big)\frac{\partial^2\psi_0}{\partial x^2}+\Big[\frac{2}{\pi}x_1c_{21}+2c_{15}(1-\nu_c)\Big]\frac{\partial^2\psi_0}{\partial y^2}+$$
$$-\Big(\frac{4}{\pi^2}x_1c_{20}+2c_{18}\Big)\frac{\partial^2\psi_1}{\partial x^2}-\Big[\frac{2}{\pi^2}x_1c_{21}+c_{18}(1-\nu_c)\Big]\frac{\partial^2\psi_1}{\partial y^2}+ \tag{3.6}$$
$$+\Big[\frac{4}{\pi}x_1\nu_f c_{20}+\frac{2}{\pi}x_1c_{21}+2c_{15}(1+\nu_c)\Big]\frac{\partial^2\phi_0}{\partial x\partial y}+$$
$$-\Big[\frac{4}{\pi^2}x_1\nu_f c_{20}+\frac{2}{\pi^2}x_1c_{21}+c_{18}(1+\nu_c)\Big]\frac{\partial^2\phi_1}{\partial x\partial y}\Big\}+$$
$$-c_{16}\psi_0+c_{19}\psi_1=0$$

$$(\delta\phi_0)\qquad \frac{2t_c^2}{1-\nu_c}\Big\{(\alpha_{12}\nu_f c_{20}+\alpha_{12}c_{21}+2c_{11})\frac{\partial^3 w}{\partial x^2\partial y}+(\alpha_{12}c_{20}+2c_{11})\cdot$$
$$\cdot\frac{\partial^3 w}{\partial y^3}-[2x_1\nu_f c_{20}+x_1c_{21}+2c_{11}(1+\nu_c)]\frac{\partial^2\psi_0}{\partial x\partial y}+$$

$$
\begin{aligned}
&+\Big[\frac{2}{\pi}x_1\nu_f c_{20}+\frac{1}{\pi}x_1c_{21}+c_{15}(1+\nu_c)\Big]\frac{\partial^2\psi_1}{\partial x\partial y}+\\
&-[x_1c_{21}+2c_{11}(1-\nu_c)]\frac{\partial^2\phi_0}{\partial x^2}-(2x_1c_{20}+4c_{11})\frac{\partial^2\phi_0}{\partial y^2}+\\
&+\Big[\frac{1}{\pi}x_1c_{21}+c_{15}(1-\nu_c)\Big]\frac{\partial^2\phi_1}{\partial x^2}+\Big(\frac{2}{\pi}x_1c_{20}+2c_{15}\Big)\frac{\partial^2\phi_1}{\partial y^2}\Big\}+\\
&+4c_0\phi_0-c_{16}\phi_1=0
\end{aligned}
\tag{3.7}
$$

$$
\begin{aligned}
(\delta\phi_1)\qquad &\frac{t_c^2}{1-\nu_c}\Big\{-\Big(\frac{2}{\pi}\alpha_{12}\nu_f c_{20}+\frac{2}{\pi}\alpha_{12}c_{21}+2c_{15}\Big)\frac{\partial^3 w}{\partial x^2\partial y}+\\
&-\Big(\frac{2}{\pi}\alpha_{12}c_{20}+2c_{15}\Big)\frac{\partial^3 w}{\partial y^3}+\\
&+\Big[\frac{4}{\pi}x_1\nu_f c_{20}+\frac{2}{\pi}x_1c_{21}+2c_{15}(1+\nu_c)\Big]\frac{\partial^2\psi_0}{\partial x\partial y}+\\
&-\Big[\frac{4}{\pi^2}x_1\nu_f c_{20}+\frac{2}{\pi^2}x_1c_{21}+c_{18}(1+\nu_c)\Big]\frac{\partial^2\psi_1}{\partial x\partial y}+\\
&+\Big[\frac{2}{\pi}x_1c_{21}+2c_{15}(1-\nu_c)\Big]\frac{\partial^2\phi_0}{\partial x^2}+\Big(\frac{4}{\pi}x_1c_{20}+4c_{15}\Big)\frac{\partial^2\phi_0}{\partial y^2}+\\
&-\Big[\frac{2}{\pi^2}x_1c_{21}+c_{18}(1-\nu_c)\Big]\frac{\partial^2\phi_1}{\partial x^2}-\Big(\frac{4}{\pi^2}x_1c_{20}+2c_{18}\Big)\frac{\partial^2\phi_1}{\partial y^2}\Big\}+\\
&-c_{16}\phi_0+c_{19}\phi_1=0
\end{aligned}
\tag{3.8}
$$

where

$$
\begin{aligned}
\alpha_{11}&=\frac{x_1(4x_1^2+6x_1+3)}{12} & \alpha_{12}&=x_1(x_1+1)\\
c_0&=1-\frac{2}{\pi}e_0 & c_{11}&=\frac{1}{12}\Big(1-6\frac{\pi^2-8}{\pi^3}e_0\Big)\\
c_{12}&=\frac{1}{\pi^2}\Big(\frac{1}{2}-\frac{8}{9\pi}e_0\Big) & c_{13}&=\frac{1}{\pi^2}\Big(\frac{1}{8}-\frac{4}{15\pi}e_0\Big)\\
c_{14}&=\frac{1}{2}-\frac{14}{15\pi}e_0 & c_{15}&=\frac{1}{4\pi^3}\Big(8-\pi e_0\Big)\\
c_{16}&=\frac{1}{\pi}\Big(4-\pi e_0\Big) & c_{18}&=\frac{1}{2\pi^2}\Big(1-\frac{4}{3\pi}e_0\Big)\\
c_{19}&=\frac{1}{2}-\frac{4}{3\pi}e_0 & c_{20}&=e_1\frac{1-\nu_c^2}{1-\nu_f^2}\\
c_{21}&=e_1\frac{1-\nu_c^2}{1+\nu_f} & c_{22}&=2\alpha_{11}c_{20}+c_{11}\\
c_{23}&=4\alpha_{11}c_{20}+2c_{11} & c_{24}&=\alpha_{12}c_{20}+2c_{11}
\end{aligned}
$$

$$c_{25}=\alpha_{12}c_{20}+2c_{11} \qquad c_{26}=\frac{1}{\pi}\alpha_{12}c_{20}+c_{15}$$
$$c_{27}=\frac{1}{\pi}\alpha_{12}c_{20}+c_{15} \qquad c_{28}=2x_1c_{20}+4c_{11}$$
$$c_{29}=x_1c_{21}+2c_{11}(1-\nu_c) \qquad c_{30}=\frac{2}{\pi}x_1c_{20}+2c_{15}$$
$$c_{31}=\frac{1}{\pi}x_1c_{21}+c_{15}(1-\nu_c) \qquad c_{32}=x_1(2\nu_f c_{20}+c_{21})+2c_{11}(1+\nu_c)$$
$$c_{34}=\frac{2}{\pi^2}x_1c_{20}+c_{18} \qquad c_{33}=\frac{1}{\pi}x_1(2\nu_f c_{20}+c_{21})+c_{15}(1+\nu_c)$$
$$c_{35}=\frac{1}{\pi^2}x_1c_{21}+\frac{1}{2}c_{18}(1-\nu_c) \qquad c_{36}=\frac{1}{\pi^2}x_1(2\nu_f c_{20}+c_{21})+\frac{1}{2}c_{18}(1+\nu_c)$$
$$c_{37}=\frac{1}{\pi}x_1c_{21}+c_{15}(1-\nu_c) \qquad e_1=\frac{E_f}{E_{c1}}$$

The boundary conditions for the simply supported sandwich plate are

$$\begin{array}{llll} w(0,y)=0 & w(a,y)=0 & w(x,0)=0 & w(x,b)=0 \\ Mg(0,y)=0 & Mg(a,y)=0 & Mg(x,0)=0 & Mg(x,b)=0 \end{array} \tag{3.9}$$

where Mg is the bending moment and w – deflection.

4. Analytical solution

There are five unknown functions in the system of stability equations. Forms of them are assumed as follows

$$\begin{array}{ll} w(x,y)=w_a\sin\frac{m\pi x}{a}\sin\frac{n\pi y}{b} & \\ \psi_0(x,y)=\psi_{a0}\cos\frac{m\pi x}{a}\sin\frac{n\pi y}{b} & \psi_1(x,y)=\psi_{a1}\cos\frac{m\pi x}{a}\sin\frac{n\pi y}{b} \\ \phi_0(x,y)=\phi_{a0}\sin\frac{m\pi x}{a}\cos\frac{n\pi y}{b} & \phi_1(x,y)=\phi_{a1}\sin\frac{m\pi x}{a}\cos\frac{n\pi y}{b} \end{array} \tag{4.1}$$

where $m,n\in N$ (N – the set of natural numbers), w_a – the amplitude of deflection, ψ_{a0}, ψ_{a1}, ϕ_{a0}, ϕ_{a1} – the amplitudes of dimensionless diceplacment functions.

These functions, Eq. (4.1) satisfy boundary conditions, Eq. (3.9). Substituting these above five functions, Eq. (4.1), into the system of stability equations (3.4)-(3.8) a system of five algebraic homogeneous equations is obtained

$$\begin{bmatrix} a_{11}-K_m & a_{12} & a_{13} & a_{14} & a_{15} \\ a_{12} & a_{22} & a_{23} & a_{24} & a_{25} \\ a_{13} & a_{23} & a_{33} & a_{25} & a_{35} \\ a_{14} & a_{24} & a_{25} & a_{44} & a_{45} \\ a_{15} & a_{25} & a_{35} & a_{45} & a_{55} \end{bmatrix} \begin{bmatrix} \dfrac{w_a}{t_c} \\ \psi_{a0} \\ \psi_{a1} \\ \phi_{a0} \\ \phi_{a1} \end{bmatrix} = \begin{bmatrix} 0 \\ 0 \\ 0 \\ 0 \\ 0 \end{bmatrix} \tag{4.2}$$

where

$$\begin{aligned}
a_{11} &= \frac{t_c^2}{a^2}(m\pi)^2[c_{22}(1+\beta^4)+c_{23}\beta^2] & a_{12} &= -\frac{t_c}{a}m\pi(c_{24}+c_{25}\beta^2) \\
a_{13} &= \frac{t_c}{a}m\pi(c_{26}+c_{27}\beta^2) & a_{14} &= -\frac{t_c}{a}m\pi(c_{24}\beta^3+c_{25}\beta) \\
a_{15} &= \frac{t_c}{a}m\pi(c_{26}\beta^3+c_{27}\beta) & a_{22} &= c_{28}+c_{29}\beta^2+2c_0c_{38} \\
a_{23} &= -\Big(c_{30}+c_{31}\beta^2+\frac{1}{2}c_{16}c_{38}\Big) & a_{24} &= c_{32}\beta \\
a_{25} &= -c_{33}\beta & a_{33} &= c_{34}+c_{35}\beta^2+\frac{1}{2}c_{19}c_{38} \\
a_{35} &= c_{36}\beta & a_{44} &= c_{29}+c_{28}\beta^2+2c_0c_{38} \\
a_{45} &= -\Big(c_{37}+c_{30}\beta^2+\frac{1}{2}c_{16}c_{38}\Big) & a_{55} &= c_{34}\beta^2+c_{35}+\frac{1}{2}c_{19}c_{38} \\
c_{38} &= \frac{a^2}{t_c^2}\frac{1-\nu_c}{(m\pi)^2} & \beta &= \frac{a}{b}\frac{n}{m} \\
K_m &= \frac{N_0}{E_{c1}t_c}[k+(1-k)\beta^2](1-\nu_c^2)
\end{aligned}$$

Because of the homogeneous algebraic equations, the main determinant of the system must be equal to zero. So, the critical forces

$$N_{0,cr} = \min_{m,n}\{N_0(m,n)\} \tag{4.3}$$

could be calculated from this equation.

5. Numerical calculations

There are some examples considered below, where the influence of the core porosity is shown for a family of plates with $b = 200\,\mathrm{mm}$, $\nu_f = 0.34$, $\nu_c = 0.15$, $E_{c1} = 7.1 \cdot 10^3\,\mathrm{MPa}$. The dimensionless parameter k is connected with the compressive forces, which means $N_x^0 = kN_0$, $N_y^0 = (1-k)N_0$, $(0 \leqslant k \leqslant 1)$.

The thickness of the core is $t_c = b/20 = 10\text{mm}$ (Figs. 3-5). The dimensionless parameter $x_1 = t_f/t_c = 1/20$ is in every example below.

In Fig. 3, the critical loads in the case $k = 1$, which means $N_x^0 = N_0$, $N_y^0 = 0$ for the plate with constant mechanical properties of the core $(e_0 = 0)$ and for the plate with varying mechanical properties of the core ($e_0 \neq 0$, $e_0 = 0,\ 0.5,\ 0.8$) and for different $e_1 = 10,\ 20,\ 30$, where $e_1 = E_f/E_{c1}$ are shown. The critical load increases when the dimensionless parameter e_1 increases or dimensionless coefficient of the core porosity e_0 decreases.

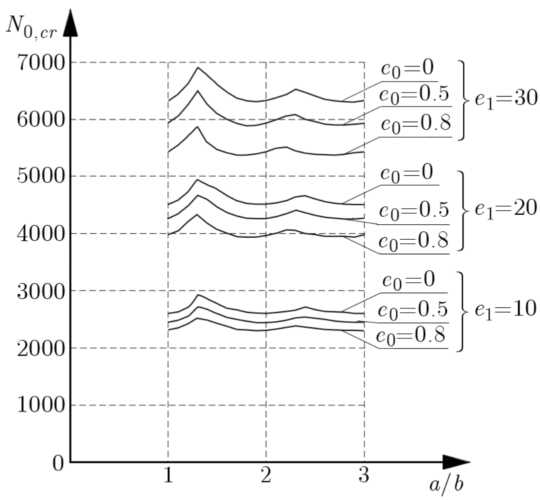

Fig. 3. Critical loads in the case $N_x^0 = N_0$, $N_y^0 = 0$, $k = 1$

In Fig. 4, the critical loads are also shown, but for different compressive forces, which means for $k = 1$, then $N_x^0 = N_0$, $N_y^0 = 0$, for $k = 0.75$, then $N_x^0 = 0.75N_0$, $N_y^0 = 0.25N_0$, for $k = 0.5$, then $N_x^0 = N_y^0 = 0.5N_0$ and for the plate with constant mechanical properties of the core $(e_0 = 0)$. In this example, the influence of dimensionless parameter e_1 is shown too. If the parameter k decreases then the critical load also decreases.

In Fig. 5, the critical loads are shown for different compressive forces ($k = 1,\ 0.75,\ 0.5$) as previously, but for the plate with varying mechanical properties of the core ($e_0 = 0.5$ in Fig. 5a and $e_0 = 0.8$ in Fig. 5b). Both of them are for the same value $e_1 = 10$.

The last two examples are for different thickness of the plate core. The dimensionless parameter $x_1 = 1/20$, so the thickness of each face also changes.

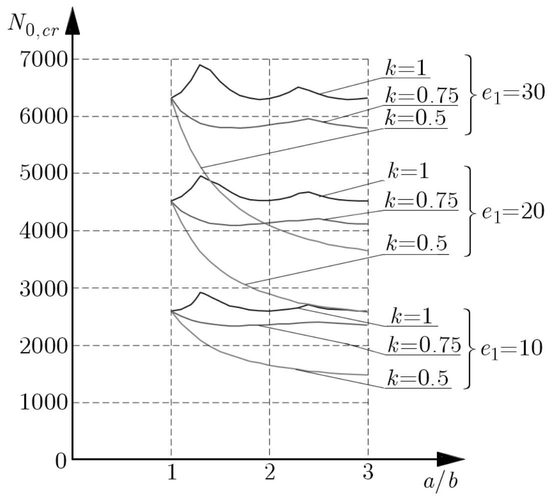

Fig. 4. Critical loads for the plate with constant mechanical properties of the core under different compressive forces; $e_0 = 0$

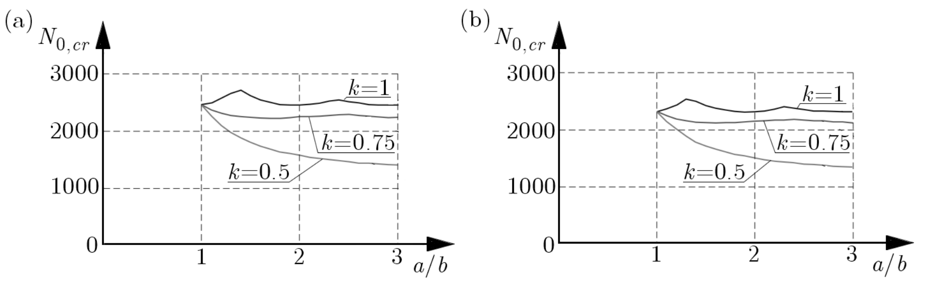

Fig. 5. Critical loads of the plate under different compressive forces; (a) $e_0 = 0.5$ $e_1 = 10$, (b) $e_0 = 0.8$ $e_1 = 10$

In Fig. 6, the influence of the thickness of the core on the critical load is shown while the parameter e_1 changes. In this example the core of the plate has constant mechanical properties $(e_0 = 0)$ and the commpresive forces are $N_x^0 = N_0,\ ,N_y^0 = 0$ $(k = 1)$.

Instead, in the last example, in Fig. 7, the influence of the thickness of the plate core for the critical load is shown, but the parameter e_1 is fixed and the coefficient of core porosity e_0 is changing.

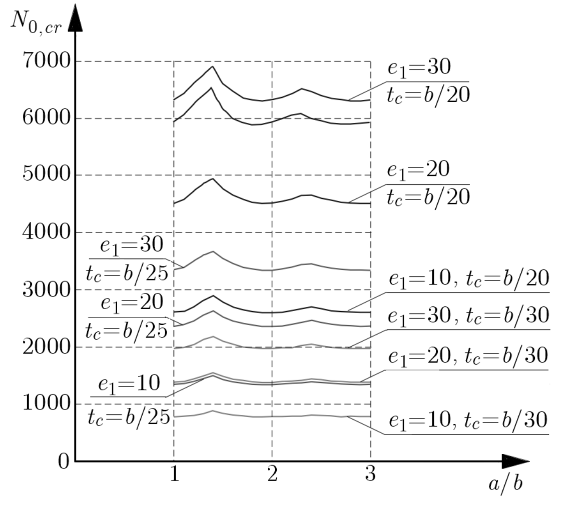

Fig. 6. Critical loads of the plate with different thickness of the core; $e_0 = 0$, $k = 1$

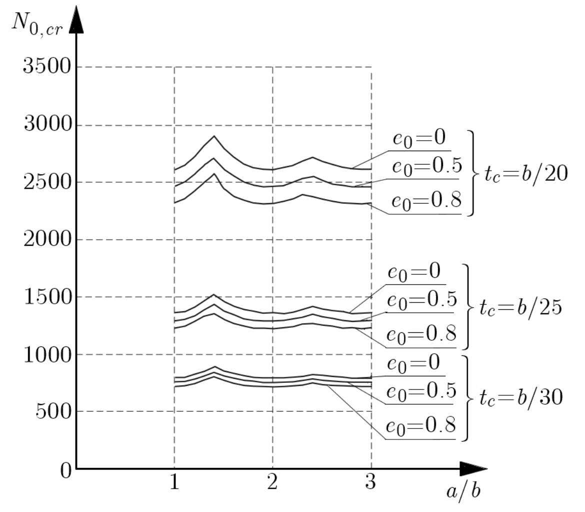

Fig. 7. Critical loads of the plate with different thickness of the core; $e_1 = 10$, $k = 1$

6. Conclusions

The field of displacements for the sandwich plate is a generalization of the classical hypotheses. The non-linear hypothesis of deformation of the plane cross section for a sandwich plate includes the shear deformable effect. The mathematical model of the sandwich plate is without internal contradiction. The equations of equilibrium-stability are correct for thin or thick plates. The system of five differential stability equations can be reduced to a single equation. The influence of the core thickness and dimensionless parameter $e_1 = E_f/E_{c1}$ on the critical load is crucial.

References

1. Apetre N.A., Sankar V., Ambur D.R., 2008, Analytical modeling of sandwich beams with functionally graded core, *Journal of Sandwich Structures and Materials*, **10**, 53-74
2. Banhart J., 2001, Manufacture, characterisation and application of cellular metals and metal foams, *Progress in Materials Science*, **46**, 559-632
3. Bart-Smith H., Hutchinson J.W., Evans A.G., 2001, Measurement and analysis of the structural performance of cellular metal sandwich construction, *Int. Journal of Mechanical Science*, **43**, 1945-1963
4. Carrera E., 2000, An assessment of mixed and classical theories on global and local response of multilayered orthotropic plates, *Composite Structures*, **50**, 183-198
5. Carrera E., 2001, Developments, ideas, and evaluations based upon Reissner's mixed variational theorem in the modeling of multilayred plates and shells, *Applied Mechanics Reviews*, **54**, 301-329
6. Carrera E., 2003, Historical review of Zig-Zag theories for multilayred plates and shells, *Applied Mechanics Reviews*, **56**, 287-308
7. Carrera E., Brischetto S., Robaldo A., 2008, Variable kinematic model for analysis of functionally graded material plates, *AIAA Journal*, **46**, 1, 194-203
8. Debowski D., Magnucki K., 2006, Dynamic stability of a porouse rectangular plate, *PAMM, Proc. Appl. Math. Mech.*, **6**, 215-216
9. Grigolyuk E.I., Chulkov P.P., 1973, *Stability and Vibrations of Three Layers Shells*, Mashinostroene, Moskow [in Russian]
10. Hohe J., Becker W., 2002, Effective stress-strain relations for two-dimensional cellular sandwich core: Homogenization, materials modes, and properties, *Applied Mechanics Reviews*, **55**, 61-86
11. Kasprzak J., Ostwald M., 2006, A generalized approach to modeling displacements in plates made of non-homogeneous materials, *XLV Sympozjon, Modelling in Mechanics*, Wisla-Poland

12. Kotełko M., Mania R., 2005, Limitations of equivalent plate approach to the load-capacity estimation of honeycomb sandwich panels under compression, *Fourth Int. Conf. Thin-Walled Structures*, J. Loughlan (Edit.), Bristol & Philadelphia: IOP Publishing, 679-686

13. Magnucka-Blandzi E., 2008, Axi-symmetrical deflection and buckling of circular porous-cellular plate, *Thin-Walled Structures*, **46**, 333-337

14. Magnucka-Blandzi E., 2009, Dynamic stability of a metal foam circular plate, *Journal of Theoretical and Applied Mechanics*, **47**, 2, 421-433

15. Magnucka-Blandzi E., 2010, Dynamic stability and static stress state of a sandwich beam with a metal foam core using three modified Timoshenko hypotheses, *Mechanics of Advanced Materials and Structures* (in print)

16. Magnucka-Blandzi E., Magnucki K., 2007, Effective design of a sandwich beam with a metal foam core, *Thin-Walled Structures*, **45**, 432-438

17. Magnucka-Blandzi E., Wasilewicz P., 2009, Strength of a rectangular sandwich plate with metal foam core, *Proceedings of the International Symposium on Cellular Metals for Structural and Functional Applications*, CELLMET 2008, G. Stephani, B. Kieback (Edit.), Fraunhofer IFAM Dresden, Germany, 283-298

18. Magnucki K., Magnucka-Blandzi E., 2006, Strength and stability of a sandwich beam with a porous-cellular core, *11-th Symposium Stability of Structures*, K. Kowal-Michalska, R.J. Mania (Edit.), Zakopane, Chair of Strength of Materials and Structures, Lodz University of Technology, 259-266

19. Magnucki K., Malinowski M., Kasprzak J., 2006, Bending and buckling of a rectangular porous plate, *Steel and Composite Structures*, **6**, 4, 319-333

20. Magnucki K., Ostwald M. (Edit.), 2001, *Stability and Optimization of Sandwich Structures*, Poznań, Zielona Góra, Wyd. Instytutu Technologii Eksploatacji w Radomiu [in Polish]

21. Magnucki K., Stasiewicz P., 2004a, Elastic bending of an isotropic porous beam, *Int. Journal of Applied Mechanics and Engineering*, **9**, 2, 351-360

22. Magnucki K., Stasiewicz P., 2004b, Elastic buckling of a porous beam, *Journal of Theoretical and Applied Mechanics*, **42**, 4, 859-868

23. Malinowski M., Magnucki K., 2005, Deflection of an isotropic porous cylindrical panel, *Proc. of the 8th SSTA Conference*, W. Pietraszkiewicz, C. Szymczak (Edit.), London, Leiden, New York, Philadelphia, Singapore: Taylor & Francis, 143-147

24. Noor A.K., Burton W.S., Bert C., 1996, Computational models for sandwich panels and shells, *Appl. Mech. Rev.*, **49**, 3, 155-199

25. Ohga M., Wijenayaka A.S., Croll J.G.A., 2005, Reduced stiffness buckling of sandwich cylindrical shells under uniform external pressure, *Thin-Walled Structures*, **43**, 1188-1201

26. Pandit M.K., Singh B.N., Sheikh A.H., 2008, Buckling of laminated sandwich plates with soft core based on an improved higher order zigzag theory, *Thin-Walled Structures*, **46**, 1183-1191

27. Plantema F.J., 1966, *Sandwich Construction: The Bending and Buckling of Sandwich Beams, Plates and Shells*, New York: John Wiley & Sons

28. Volmir A.S., 1967, *Stability of Deformation Systems*, Moscow: Nauka, Fizmatlit [in Russian]

29. Wang C.M., Reddy J.N., Lee K.H., 2000, *Shear Deformable Beams and Plates*, Elsevier, Amsterdam, Lousanne, New York, Oxford, Shannon, Singapore, Tokyo

Matematyczne modelowanie prostokątnej płyty trójwarstwowej z rdzeniem z pianki metalowej

Streszczenie

Przedmiotem pracy jest prostokątna płyta trójwarstwowa podparta przegubowo na czterech brzegach i ściskana w płaszczyźnie środkowej. Okładziny płyty są izotropowe i o takich samych właściwościach mechanicznych. Rdzeń wykonany z pianki metalowej jest również izotropowy, jego właściwości mechaniczne są zmienne na grubości. Płaszczyzna środkowa płyty jest jej płaszczyzną symetrii. Zdefiniowano pole przemieszczeń dla dowolnego punktu rdzenia oraz okładzin płyty. Sformułowano energię odkształcenia sprężystego płyty i pracę obciążenia. Następnie z zasady stacjonarności całkowitej energii potencjalnej otrzymano układ równań równowagi, który rozwiązano analitycznie w sposób przybliżony i wyznaczono obciążenie krytyczne płyty.

Manuscript received July 5, 2010; accepted for print November 22, 2010